JOURNAL OF SOLID STATE CHEMISTRY **129,** 287–297 (1997)
ARTICLE NO. SC967248

Vibrational Characteristics of the Alkali Metal–Indium Double Molybdates $M\text{In}(\text{MoO}_4)_2$ and Tungstates $M\text{In}(\text{WO}_4)_2$ (M=Li, Na, K, Cs)

M. Mączka

Institute of Low Temperature and Structure Research, Polish Academy of Sciences, Wrocław, Poland

Received April 17, 1996; in revised form November 25, 1996; accepted November 27, 1996

Infrared and Raman spectra of polycrystalline alkali metal–indium double molybdates $M\text{In}(\text{MoO}_4)_2$ (where M = Na, K, Cs) and alkali metal-indium double tungstates $M\text{In}(\text{WO}_4)_2$ (where M = Li, Na, K) were measured in the range 40–1000 cm^{-1} at room temperature. To determine the symmetries and nature of the observed modes a factor group analysis has been performed. The crystal structure of the compounds studied depends on the type of cation and changes from trigonal (for the caesium–indium molybdate) to monoclinic and triclinic (for the lithium and sodium derivatives). The character of the coordination sphere around the molybdenum and tungsten atoms changes from tetrahedral (for the studied double molybdates and $K\text{In}(\text{WO}_4)_2$) to octahedral (for the $\text{LiIn}(\text{WO}_4)_2$ and $\text{NaIn}(\text{WO}_4)_2$). The assignment of the observed bands to the respective internal and external vibrational modes is proposed.

1. INTRODUCTION

Double molybdates and tungstates have been extensively studied for many years since they are suitable as host materials for a variety of inorganic phosphors. The properties of alkali metal–bismuth double molybdates and tungstates have been the subject of our previous studies (1–5). Alkali metal–indium double molybdates and tungstates belong to another group of promising laser materials. These crystals can be easily doped with chromium(III) ions and the coordination of the chromium ions is near octahedral. To understand the electronic properties of indium compounds doped with chromium ions it is important to know the vibrational level distribution of the host materials, their symmetries, and assignment to the respective normal modes. In the present paper the dependence of the vibrational properties on the structural arrangement for three molybdates and three double tungstates are discussed.

The caesium–indium double molybdate was obtained in two structural modifications, trigonal and orthorhombic. Although the phase transition temperature from the trigonal to the orthorhombic structure is 743 K (6), it is possible to obtain the high-temperature modification at room temperature by fast cooling. The dependence of the crystal structure on the cooling rate was observed earlier for $\text{RbIn}(\text{MoO}_4)_2$ (7).

2. EXPERIMENTAL

The compounds studied have been grown by the thermal method developed by Borisov and Klevtsova (8) and Klevtsov *et al.* (9). $\text{CsIn}(\text{MoO}_4)_2$ has been obtained by heating the stoichiometric mixture of Cs_2CO_3, In_2O_3, and MoO_3, to 650°C and keeping it at this temperature for 48 h. To obtain the trigonal modification the mixture was cooled down to room temperature with the rate 5°C per min. In the case of the orthorhombic structure the cooling rate was 2°C per h.

Powder diffraction spectra were measured by a Stoe powder diffraction system, using Cu$K\alpha$ radiation. IR spectra in nujol and KBr suspensions at 300 K were recorded with a Perkin–Elmer 2000 FT-IR spectrophotometer. Raman spectra were measured in back-scattering geometry with a Perkin–Elmer 2000 near-infrared FT-Raman spectrometer. The excitation source was the 1064 nm line of a YAG: Nd^{3+} laser. The laser output power was 150 mW. Since the InGaAs detector was not able to measure Raman spectra below 200 cm^{-1}, the spectra in the range 250–50 cm^{-1} were recorded with a double-beam DFS 24 monochromator with a photon counting system (cooled GaAs Burle (USA) photomultiplier). The IR spectra in the region 450–1000 cm^{-1} and Raman spectra in the region 200–1000 cm^{-1} were recorded with 1 cm^{-1} spectral resolution. The far-infrared and Raman spectra in the range 250–40 cm^{-1} were measured with 2 and 4 cm^{-1} resolution, respectively.

3. RESULTS AND FACTOR GROUP ANALYSIS (FGA)

3.1. *Molybdate with Triclinic Structure* ($NaIn(MoO_4)_2$)

$\text{NaIn}(\text{MoO}_4)_2$ crystallizes in the triclinic $P\bar{1} = C_i^1$ structure. The unit cell of this crystal contains four formula units and the lattice parameters are: $a = 7.18$, $b = 7.18$, $c = 14.90$ Å, $\alpha = 92$, $\beta = 88$, and $\gamma = 82°$ (10) . The MoO_4^{2-} tetrahedra in the structure of $\text{NaIn}(\text{MoO}_4)_2$ occupy four and cations two crystallographically nonequivalent sites of

0022-4596/97 $25.00

C_1 symmetry. According to the factor group analysis a total of 144 unit-cell modes are distributed among $3A_u$ acoustic modes, $24A_g + 21A_u$ translational modes, $12A_g + 12A_u$ librational modes, and $36A_g + 36A_u$ internal modes. The vibrational frequencies are listed in Table 1 and the spectra are presented in Fig. 1.

3.2. Compounds with the Orthorhombic Structure ($KIn(MoO_4)_2$, $CsIn(MoO_4)_2$ and $KIn(WO_4)_2$) and the Trigonal $CsIn(MoO_4)_2$ Modification

The potassium–indium double molybdate crystallizes in the orthorhombic structure, space group $Pnam = D_{2h}^{16}$ and

TABLE 1
Vibrational Wavenumbers for Polycrystalline $NaIn(MoO_4)_2$, $KIn(MoO_4)_2$, and $KIn(WO_4)_2$

$NaIn(MoO_4)_2$		$KIn(MoO_4)_2$		$KIn(WO_4)_2$		
IR spectrum	Raman spectrum	IR spectrum	Raman spectrum	IR spectrum	Raman spectrum	Assignments
983w	982s	973m	967sh	992m	988w	$\nu_s(MO_4)$
975w	972s	958sh	963m	980m	975vs	
957m	947s	949sh	956m			
941m	938w	939sh	941vs			
931m	927m	931s	935sh	960sh		$\nu_{as}(MO_4)$
	922sh		915m	940s	949w	
901w	894w	891w	881m	908w	910s	
	882m			890w	892w	
873sh	874vw			874w	885m	
859sh	856w	860w		859sh	850vw	
842sh	831m	837sh	838w			
824s	826sh	802s	814w	822s		
811sh			798w	810s	779m	
786m	770w		767m	762w	764m	
758m	759w	740w	748m			
	738w					
462m	439w					$\delta_{as}(MO_4)$
429m	419w					
404m	398m	406m	407w	398s	405w	
393sh		386m	377m		373s	
381sh	379m		357m	355w		$\delta_s(MO_4)$
	345sh	344m	346s	344s	348s	
	339sh					
335sh	334s			330sh	336w	
328w	325s	327w	331s			
315sh	319sh	323sh	321w			
311w				302s	316w	
297w	294w	302w	298w			
281w		278w				
276sh	271w			275s	287w	
270sh	267w	266m	266w		261w	
252w						$T'(In^{3+})$, $T'(Na^+)$ and $T'(K^+)$
224w	228w	220m	223w	215w	222w	
201w	217vw	206sh			214w	
197sh		175w	183w	202vw	204w	
178w		160s	168w	181sh	172m	
160w	165w			164s	158w	
	155w					
146m	148sh					
140sh	140m	144s	147w	143m	144m	$L(MoO_4^{2-})$ and $L(WO_4^{2-})$
		139sh		138m	127w	
	127w	118w	115sh	111w	111w	$T'(MoO_4^{2-})$ and $T'(WO_4^{2-})$
				101w	99w	
107m	102m	100m	108m	90w	91m	
	92w	82w	84w		87m	
	82m	49m	71w	71w	84m	

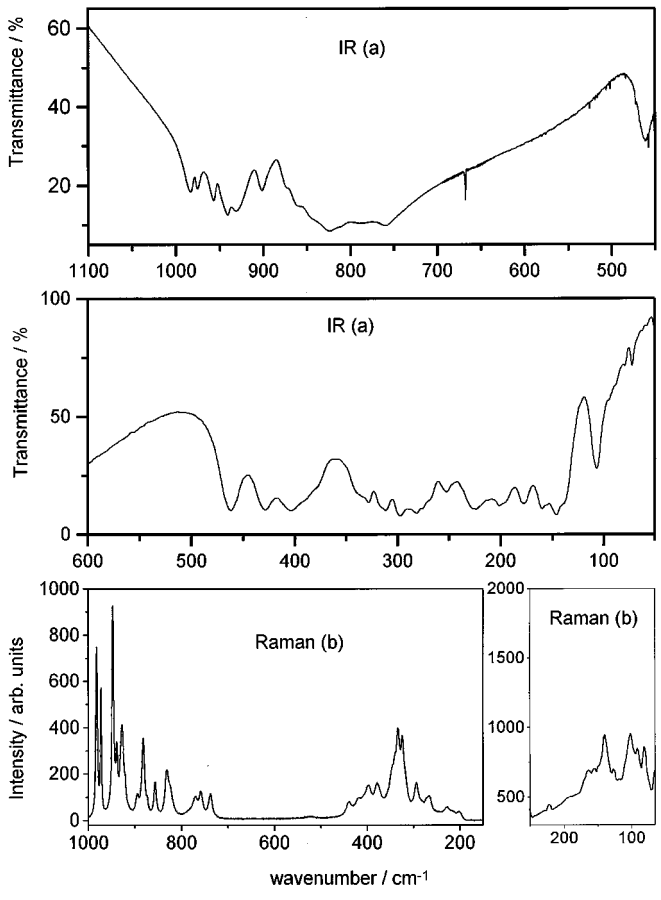

FIG. 1. IR (a) and Raman (b) spectra of $NaIn(MoO_4)_2$.

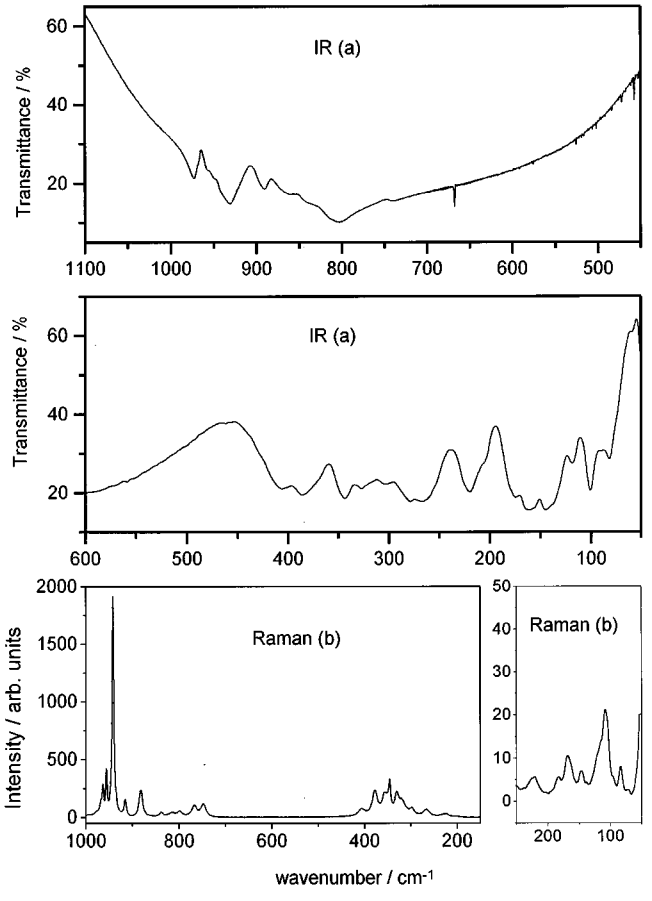

FIG. 2. IR (a) and Raman (b) spectra of $KIn(MoO_4)_2$.

lattice parameters $a = 14.79$, $b = 8.729$, $c = 5.879$ and $Z = 4$ (11). In this structure all the cations are crystallographically equivalent and occupy sites of C_s symmetry. The molybdate ions form two sets of crystallographically nonequivalent sites of C_s symmetry. According to Klevtsov *et al.* (11), the $KIn(MoO_4)_2$ crystal exhibits no phase transition between the room- and the melting-point temperature ($840^\circ C$). There are 144 zone-center modes, 3 of which are acoustic ($B_{1u} + B_{2u} + B_{3u}$), 45 translational ($8A_g + 4B_{1g} + 8B_{2g} + 4B_{3g} + 4A_u + 7B_{1u} + 3B_{2u} + 7B_{3u}$), 24 librational ($2A_g + 4B_{1g} + 2B_{2g} + 4B_{3g} + 4A_u + 2B_{1u} + 4B_{2u} + 2B_{3u}$), and 72 internal modes ($12A_g + 6B_{1g} + 12B_{2g} + 6B_{3g} + 6A_u + 12B_{1u} + 6B_{2u} + 12B_{3u}$). The wavenumbers of the observed vibrational modes and their assignments are presented in Table 1. The recorded spectra are shown in Fig. 2.

According to the literature data the $KIn(WO_4)_2$ crystal may be obtained in a few different structural modifications. The trigonal, $P\bar{3}m1$ structure (with $a = 5.80$, $c = 7.25$ Å, and $Z = 1$) exists in the 850–930°C temperature range (7, 12, 13). It was possible to freeze this high-temperature phase down to room temperature by putting hot sample into the water (13). Later, a new phase transition was discovered in the trigonal phase at the temperature 181°C (14, 15). This ferroelastic phase transition has been a subject of many EPR and crystallographic studies (16–19). It was shown that the structure below $181^\circ C$ is monoclinic ($C2/c = C_{2h}^6$, $a = 10.11$, $b = 5.78$, $c = 14.49$, $\beta = 90.33^\circ$ (15)). When the trigonal $KIn(WO_4)_2$ crystal is slowly cooled (i.e., a few degree per hour) it exhibits a phase transition at 850°C to the orthorhombic, $KIn(MoO_4)_2$-type structure ($Pnam = D_{2h}^{16}$, $a = 14.75$, $b = 8.74$, $c = 5.90$ Å, $Z = 4$) (7). Kharchenko *et al.* (12) concluded that this orthorhombic structure is stable in the 730–860°C temperature range and below 730°C the structure is monoclinic, α-$KY(WO_4)_2$-type ($C2/c$, $a = 8.14$, $b = 10.08$, $c = 7.38$ Å, $\beta = 94^\circ$, and $Z = 4$). This low-temperature structure was, however, obtained only with the hydrothermal method, where the reaction temperature (550–500°C) was below that of the orthorhombic–monoclinic phase transition (12).

In the present studies the crystals were obtained by the thermal method with the cooling rate of 2°C per hour. The recorded powder diffraction and vibrational spectra (Fig. 3, Table 2) indicate that the obtained crystals are

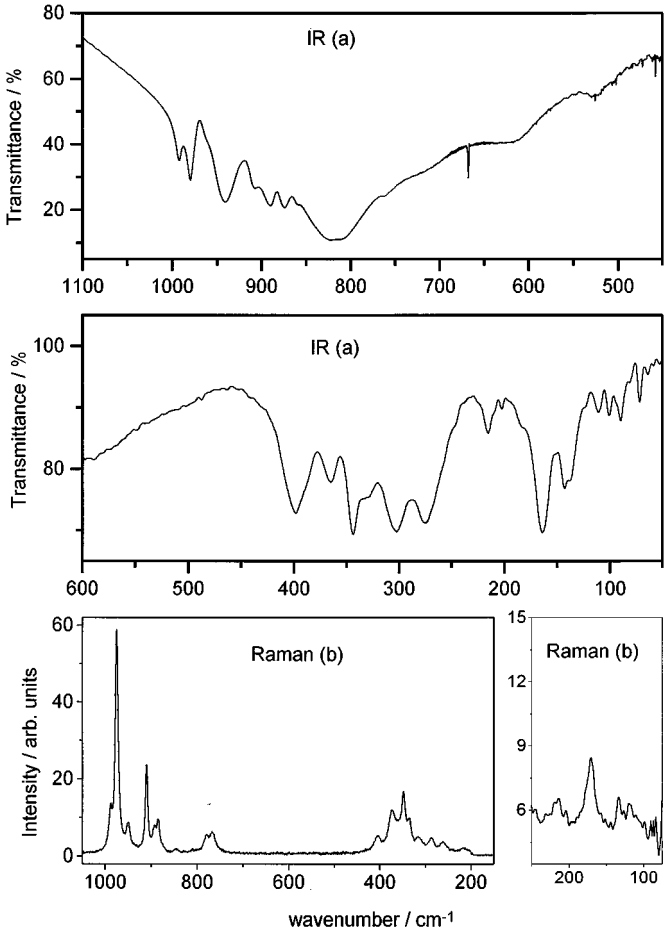

FIG. 3. IR (a) and Raman (b) spectra of $KIn(WO_4)_2$.

TABLE 2
X-Ray Powder Diffraction Data for the Trigonal and Orthorhombic $CsIn(MoO_4)_2$ and Orthorhombic $KIn(WO_4)_2$

$CsIn(MoO_4)_2$				$KIn(WO_4)_2$	
trigonal		orthorhombic			
d (Å)	intensity	d (Å)	intensity	d (Å)	intensity
5.026	47.0	4.735	11.4	4.625	48.9
4.271	68.9	4.037	9.7	4.071	34.9
3.152	100.0	3.667	47.7	3.749	100.0
2.893	88.1	3.502	16.5	3.469	29.9
2.392	10.1	3.424	15.7	3.410	13.3
2.131	34.9	3.322	18.4		
1.843	15.5	3.236	44.1	3.169	36.7
1.719	29.6	3.045	9.9	3.125	29.8
1.673	15.5	2.935	100.0	2.943	69.2
1.662	17.4	2.782	8.1	2.799	9.6
1.578	6.8	2.744	10.3	2.741	14.1
1.553	6.5	2.682	7.7		
1.449	14.6	2.556	15.6	2.577	21.7
		2.470	21.4		
		2.357	18.7		
		2.288	10.3		
		2.234	9.4		
		2.174	10.7	2.034	20.6
		2.007	9.8		
		1.975	6.9		
		1.902	9.7	1.888	16.0
		1.809	13.0	1.843	12.4
		1.792	11.3	1.786	17.4
		1.764	21.3	1.755	10.1
				1.734	13.8
		1.628	11.5	1.681	9.0
		1.581	10.0	1.583	9.6

orthorhombic and isostructural to those of $KIn(MoO_4)_2$. No α-$KY(WO_4)_2$-type crystals were obtained.

Caesium–indium double molybdate crystallizes also in the orthorhombic structure, for which the lattice parameters are $a = 14.79$, $b = 8.729$, and $c = 5.879$ Å (6). This compound can be, however, easily obtained also in the trigonal structure (space group $P\bar{3}m1 = D_{3d}^3$, $a = 5.839$, $c = 8.103$ Å, $Z = 1$ (6)). In the trigonal structure the MoO_4^{2-} tetrahedra occupy the specific position $2d_1$ with symmetry C_{3v}. The In^{3+} and Cs^+ cations occupy the positions $1a$ and $1b$ with symmetry D_{3d}. The one molecule in the trigonal unit cell gives rise to 36 vibrational modes: $A_{2u} + E_u$ acoustic, $A_{1g} + E_g + 2A_{2u} + 2E_u$ translational, $A_{2g} + E_g + A_{1u} + E_u$ librational, and $3A_{1g} + 3E_g + 3A_{2u} + 3E_u$ internal modes. The diagram which correlates the internal and librational modes of the molybdate ion with the respective modes of the trigonal and orthorhombic crystals is presented in Table 3. The IR and Raman spectra measured for both modifications (Figs. 4 and 5, Table 4) show that the symmetry lowering during phase transition (from the trigonal to the orthorhombic structure) results in the splitting of the observed bands into a few components. Moreover, some of the IR and Raman inactive modes, for the trigonal crystal, become active for the low-temperature modification.

3.3. *Monoclinic Tungstate of the $C2/c = C_{2h}^6$ Structure ($LiIn(WO_4)_2$)*

The $LiIn(WO_4)_2$ crystallizes in the monoclinic structure $C2/c = C_{2h}^6$ (20, 21). The unit-cell dimensions are as follows: $a = 9.57$, $b = 11.59$, $c = 4.95$ Å, $\beta = 91.1^\circ$, and $Z = 4$ (20). The crystal is built up of WO_4^{2-} ions connected to each other by means of intermolecular interactions of

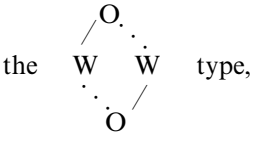

the type,

TABLE 3
Correlation Diagram for the Trigonal and Orthorhombic $CsIn(MoO_4)_2$ Crystals

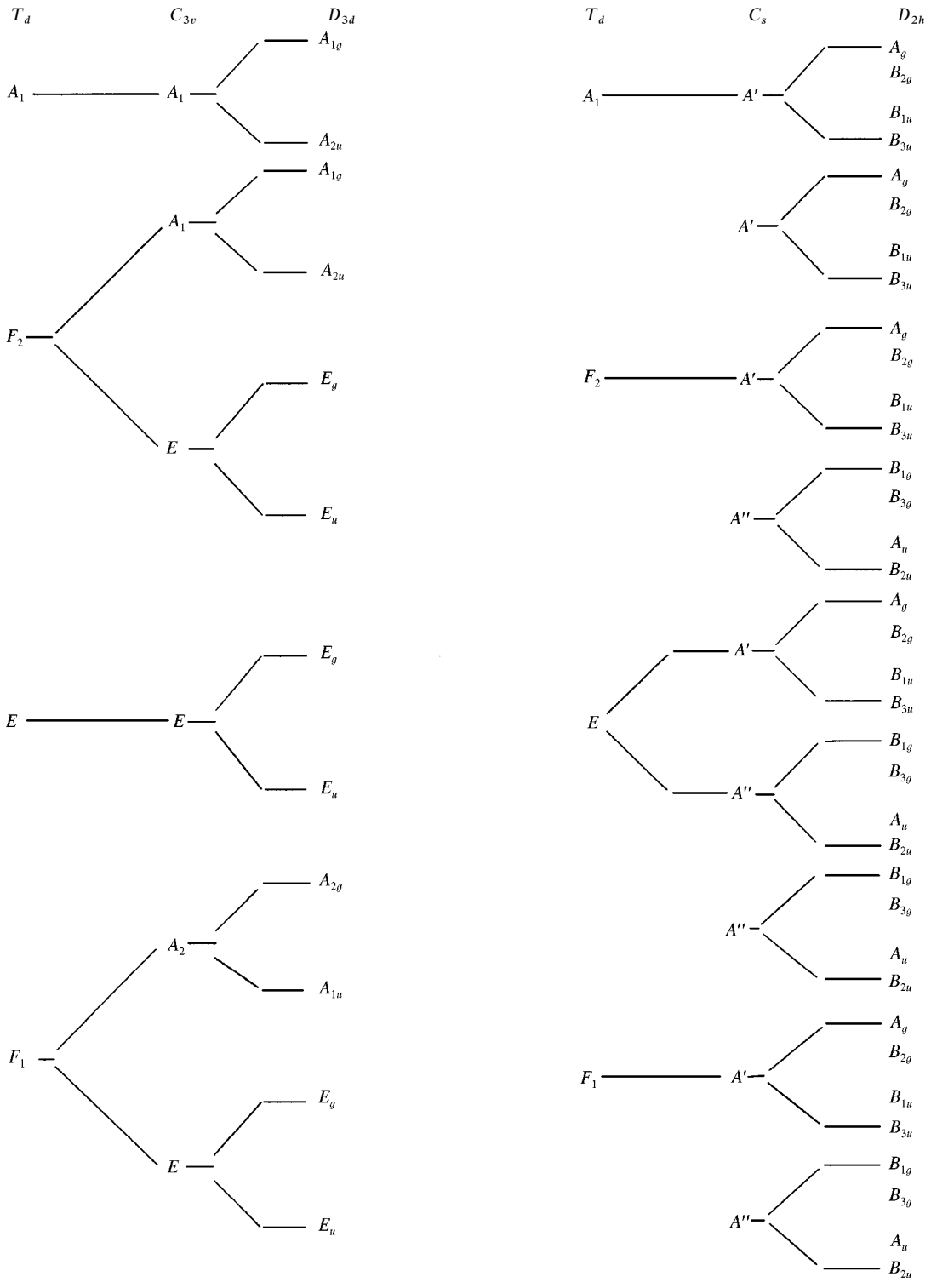

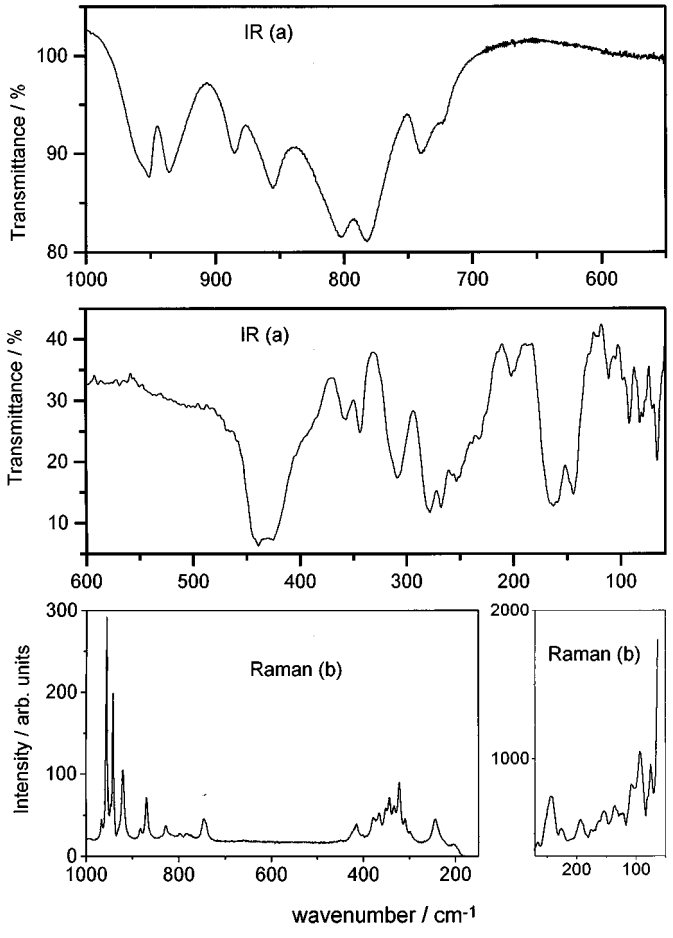

FIG. 4. IR (a) and Raman (b) spectra of the orthorhombic $CsIn(MoO_4)_2$.

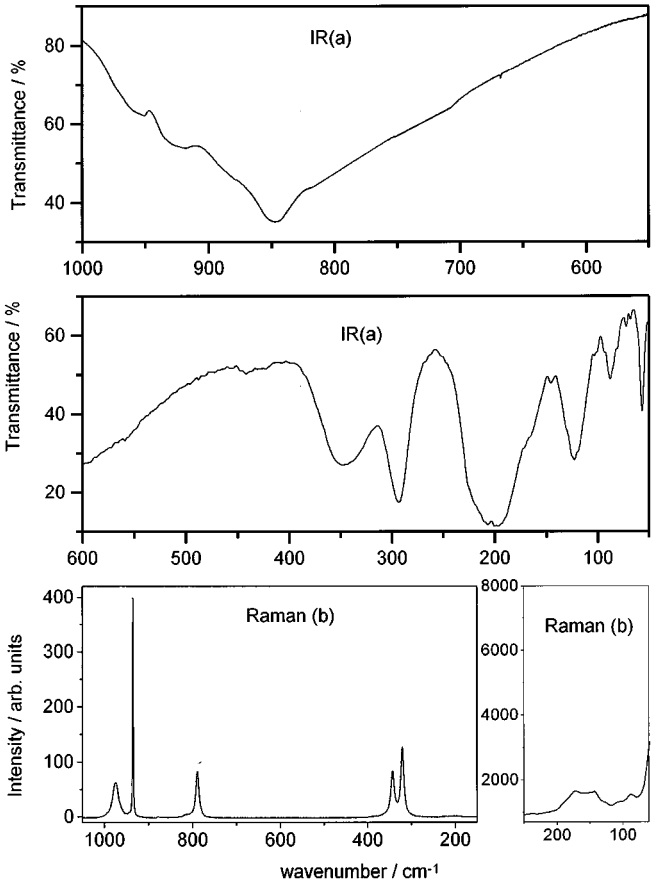

FIG. 5. IR (a) and Raman (b) spectra of the trigonal $CsIn(MoO_4)_2$.

forming chains along the c direction. The two different W···O distances are 2.36 and 2.07 Å. The

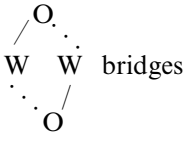

are related to each other by a c glide plane and the double oxygen bridge symmetry is C_1. All oxygen bridges in the crystal are crystallographically equivalent and the resulting coordination of the tungstate atoms is octahedral. According to the FGA the three acoustic modes are distributed among $A_u + 2B_u$, translational among $4A_g + 5B_g + 2A_u + 4B_u$, librational among $A_g + 2B_g + 2A_u + B_u$, and internal among $12A_g + 12B_g + 12A_u + 12B_u$ irreducible representations. The recorded spectra (Fig. 6, Table 5) differ significantly from those of the above-described molybdates.

The new bands are observed in the region 450–700 cm^{-1} due to the

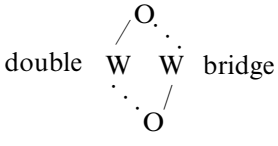

vibrations.

3.4. *Monoclinic Tungstate of $P2_1/c$ Structure ($NaIn(WO_4)_2$)*

$NaIn(WO_4)_2$ crystallizes in the $P2/c$ structure with $a = 10.077$, $b = 5.808$, $c = 5.027$ Å, and $\beta = 91.10^\circ$ (21–25). This structure is very similar to that of the $LiIn(WO_4)_2$. Also in this case the crystal is built up of tungstate chains. Since the unit cell contains only two formula units the results of the FGA are the same as for the $LiIn(WO_4)_2$. The $NaIn(WO_4)_2$ structure differs significantly, however, from that of lithium–indium double tungstate: there exist in the $NaIn(WO_4)_2$ crystal two different kinds of oxygen bridges.

TABLE 4
Vibrational Wavenumbers for Orthorhombic (*Pnam*) and Trigonal ($P\bar{3}m1$) $CsIn(MoO_4)_2$

IR spectra		Raman spectra		
Pnam	$P\bar{3}m1$	*Pnam*	$P\bar{3}m1$	Assignments
		966w		
958sh	956sh	956s	974m	$\nu_s(MoO_4)$
951m		947vw		
		941s		
936m	914sh	920m	935s	
885w		883w		
855m	846s	869m		
802s		827w		$\nu_{as}(MoO_4)$
781s		798w	789m	
739m		743m		
		741sh		
440s		423sh		
427s		416w		
		377m		$\delta_{as}(MoO_4)$
		366m		
358m		352w		
344m	344s	343m	343m	
		334w		
		322m	321m	
306s	293s	310w		$\delta_s(MoO_4)$
284s		297vw		
269w				
253w				
230m		243m		
226m	206s	222w		$T'(In^{3+})$
203m	196s	193w		
167s		175w		
		154w	173m	
		150w	148m	
145m	123s	140w		$L(MoO_4)$ and $T'(MoO_4)$
		136w		
		125w		
111w		119w		
		109w		
		94m		$T'(Cs^+)$
92w	88w	90m		
81w		77m		
		73m	88w	
66w		63w		$T'(MoO_4)$
51w	57m	57w		
44w				

In one type of the bridge the two W···O distances are 2.09 Å and for the other they are 2.24 Å. These differences in the crystal structures of the both compounds are clearly visible in the vibrational spectra (Fig. 7, Table 5).

4. DISCUSSION

4.1. X-Ray Analysis

The purity and structure of all compounds studied were checked by X-ray powder diffraction. The recorded X-ray patterns for the $NaIn(MoO_4)_2$, $KIn(MoO_4)_2$, $LiIn(WO_4)_2$, $NaIn(WO_4)_2$, and $KIn(WO_4)_2$ compounds agree very well with those published earlier (10, 11, 22, 26). No literature data concerning powder diffraction spectra are available for the orthorhombic and the trigonal modifications of $CsIn(MoO_4)_2$. The number of the observed diffraction lines (Table 4) and the *hkl* distances for the orthorhombic sample are very similar to those of the isomorphic $KIn(MoO_4)_2$ crystal. The powder diffraction pattern of the trigonal caesium–indium double molybdate is similar to those of other trigonal molybdates ($KSc(MoO_4)_2$ (27) and $CsSc(MoO_4)_2$ (28)).

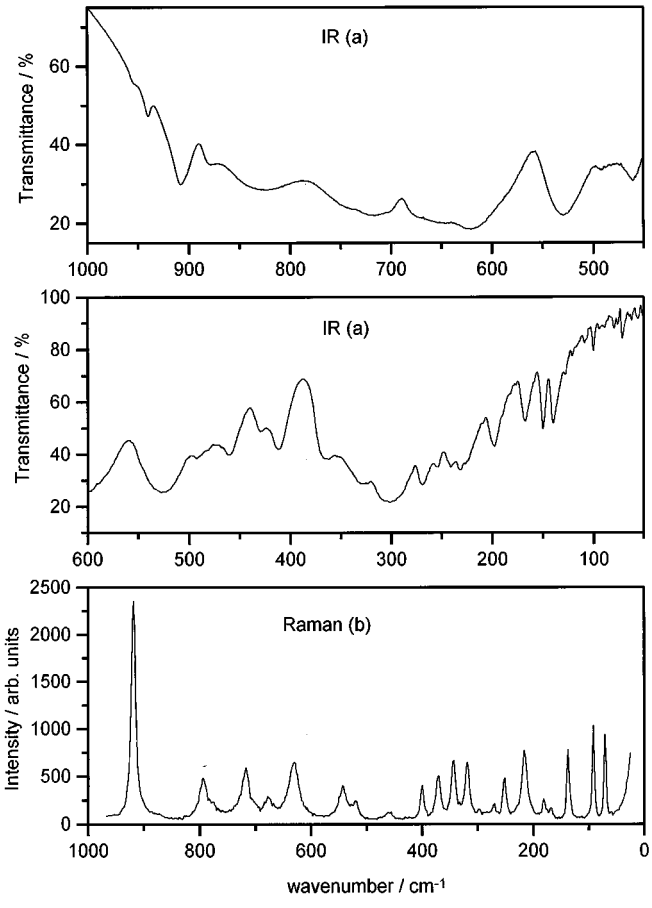

FIG. 6. IR (a) and Raman (b) spectra of $LiIn(WO_4)_2$.

4.2. Internal Vibrations

Studies of the MoO_4^{2-} anion in aqueous solutions have located its fundamental frequencies at 894 ($\nu_1(A_1)$), 318 ($\nu_2(E)$), 833 ($\nu_3(F_2)$), and 407 cm^{-1} ($\nu_4(F_2)$) (29). The respective vibrational modes of the WO_4^{2-} tetrahedra have been observed at 928, 320, 833, and 405 cm^{-1} (30). Studies of the solid compounds (31–45) have shown that the stretching

TABLE 5
Vibrational Wavenumbers for Polycrystalline $LiIn(WO_4)_2$ and $NaIn(WO_4)_2$

$NaIn(WO_4)_2$		$LiIn(WO_4)_2$		
IR spectrum	Raman spectrum	IR spectrum	Raman spectrum	Assignments
963s	974vs	940w		ν_s(W–O)
940s	936m	908m	916s	
	834m	825s	793m	ν_{as}(W–O)
791s	797w		775	
		738sh		
712m	716m	716s	716m	ν(W–O–W)
	698w	648sh	675w	
605s	621m	621s	626m	
522m	541m	528s	541m	
507w			528sh	
477w	498w	491vw		
453m	458w	460m	457w	
404m	402m	430w		
371w	366sh	412m	396m	δ(W–O) and $T'(Li^+)$
	353m	364w	368m	
332s	323vw		340m	
	304m	327w	315m	
293s	288w	301s	295vw	
	270w	269w	268vw	
	265sh	254vw	248m	δ(W–O–W) and $T'(Na^+)$
247s	239w	241m		
217w	213m	231m		
		226sh	213m	
185m	193sh	198m	178w	
167m	166m	167m	166vw	$T'(In^{3+})$
150w		150m		
146w				
136w	138sh			
129m	120m	140m	135m	
100vw				
92m	87m	100w	89m	$T'(WO_6)$ and $L(WO_6)$
80w				
71m		71w	68m	
57w				

multiplets (ν_1 and ν_3) occur in the 750–1000 cm^{-1} range and the bending modes in the 250–430 cm^{-1} range for molybdates and tungstates where anions form isolated tetrahedra. The situation is complicated when the coordination of Mo (or W) atoms is octahedral. The characteristic feature of the hexa-coordinated compounds is appearance of new bands in the region 500–750 cm^{-1}, due to the oxygen bridge bond vibrations (35, 46–48).

In the present studies all double molybdates and the potassium-indium double tungstate are composed of isolated tetrahedra (MoO_4^{2-} or WO_4^{2-}). Only one symmetric ($A_{1g} + A_{2u}$) and two asymmetric stretching modes ($A_{1g} + E_g + A_{2u} + E_u$) should be observed both in IR and Raman spectrum of the trigonal $CsIn(MoO_4)_2$. The recorded spectra are in agreement with these predictions (Fig. 5). Of the three observed bands the medium intensity Raman band at 789 cm^{-1} and strong IR band at 846 cm^{-1} originate from asymmetric vibration of MoO_4^{2-} tetrahedra since according to intensity considerations (Müller *et al.* (49)) the ν_3 has higher intensity than ν_1 in IR spectra and the reverse holds in Raman measurements. The second asymmetric stretching mode is more difficult to locate since both IR bands at 956 and 914 cm^{-1} are weak. In the Raman spectrum the strongest and narrow band is observed at 935 cm^{-1} and the second, much weaker and broader, at 974 cm^{-1}. The former band could be assigned to the symmetric stretching vibration and the second to the asymmetric stretching vibration. However, in my former study of trigonal $KSc(WO_4)_2$ and $CsSc(WO_4)_2$ (50) the bands around 930 cm^{-1} are much weaker and broader and the strongest Raman bands are those around 1000 cm^{-1}. Therefore, I assigned the 974 cm^{-1} band to ν_1 and the 935 cm^{-1} band to the ν_3 mode. The vibrational spectra of the orthorhombic $CsIn(MoO_4)_2$ support this assignment. For this crystal the ν_1 mode is expected to split into eight

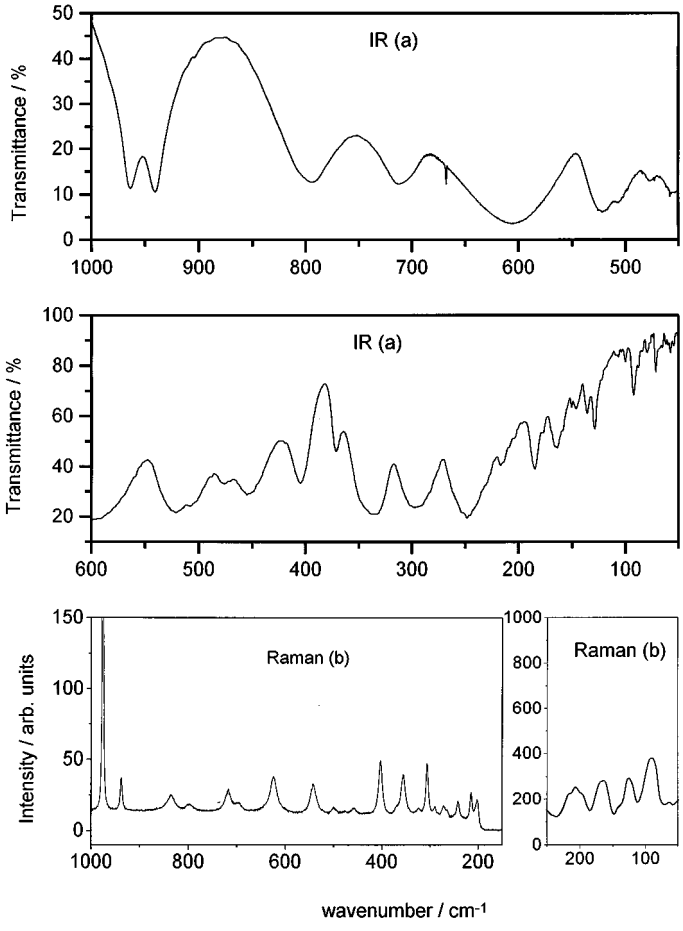

FIG. 7. IR(a) and Raman (b) spectra of $NaIn(WO_4)_2$.

components ($2A_g + 2B_g + 2B_{1u} + 2B_{3u}$). The A_g and B_g modes are Raman and B_{1u} and B_{3u} are IR active. The Raman bands at 956 and 941 cm^{-1} are very intense and therefore they can be assigned to totally symmetric stretching modes (A_g). The IR spectrum consists in this region of one band at 951 cm^{-1} with a shoulder at 958 cm^{-1}. The observation of only two IR modes indicates on a very small Davydov splitting in this compound and therefore for the polycrystalline sample each $B_{1u} + B_{3u}$ pair is observed as one band. The asymmetric stretching modes are observed as weak and medium intensity Raman bands and medium to strong intensity IR bands, in agreement with the intensity rule. Of 12 predicted Raman and 10 IR active modes only 7 are recorded in Raman and 6 in the IR spectrum since for the majority of modes no factor group splitting is observed. The number of observed vibrational modes is smaller than predicted also for the other orthorhombic crystals, $KIn(MoO_2)_4$ and $KIn(WO_4)_2$. Four symmetric modes are observed both in Raman and IR spectra of the $KIn(MoO_4)_2$ and only two for the double tungstate. The respective asymmetric modes, observed in the range 740–940 cm^{-1}, give rise to strong IR and weak Raman bands. In the case of the $NaIn(MoO_4)_2$, crystallizing in triclinic structure, 4 symmetric and 12 asymmetric vibrational modes should be observed in both Raman and IR spectrua. The four components of the ν_1 vibration are easily located in the range 938–983 cm^{-1} since the recorded Raman bands are strong. Of the 12 asymmetric modes, only 1 is missing in Raman and 3 in the IR spectrum. This is probably due to either accidental degeneracy or to overlapping of some bands by much stronger ones. The vibrational characteristics of the compounds studied depends strongly on the nature of the anion and the crystalline structure. Both ν_1 and ν_3 modes are observed at higher wavenumbers (992–975 and 960–762 cm^{-1}, respectively) for the double tungstate in comparison with the double molybdates (983–938 and 936 − 738 cm^{-1}). The lowering of crystal symmetry from trigonal to triclinic results in splitting of the 1 ν_1 vibrational level into 4 and the 2 ν_3 levels into 11 components.

The bending vibrations are observed in the 253–462 cm^{-1} wavenumber region. The statement that $\nu_4 > \nu_2$ (49) is not completely fulfilled. In some cases the ν_4 and ν_2 vibrations are well separated and observed as two groups of bands. For $NaIn(MoO_4)_2$, ν_4 bands are observed at 379-462 and ν_2 at 267–345 cm^{-1}. For the orthorhombic compounds, however, Raman spectra consist of many sharp bands and no clear separation between ν_2 and ν_4 modes can be observed. For these crystals some of the lowest ν_4 components may fall below the highest ν_2 ones. The situation is also not clear in the case of the trigonal $CsIn(MoO_4)_2$. As a result of symmetry lowering from T_d for a regular, isolated tetrahedra to C_{3v} in the trigonal crystal, the $\nu_4(F_2)$ vibration should be split into two components (E_g and A_{1g} in Raman and A_{2u} and E_u in IR). Therefore, together with the ν_2 mode, three bands are expected to be observed in the bending mode region. However, both the IR and Raman spectra consist in this region of two bands only. A similar spectroscopic feature was observed also for the $KSc(MoO_4)_2$ crystal (51) where the 351 cm^{-1} Raman active band was assigned to $\nu_2(E_g)$ mode and the 328 cm^{-1} one to $\nu_4(E_g + A_{1g})$). The respective IR active modes were located at 363 cm^{-1} ($\nu_2(E_u)$ and 292 cm^{-1} (ν_4 ($E_u + A_{2u}$)). This assignment seems, however, to be incorrect. All studies concerning simple and double molybdates indicate that the strongest Raman lines are observed about 320 cm^{-1} and are due to symmetric bending vibrations (ν_2). Therefore, it is most likely that the 321 cm^{-1} Raman line originate from ν_2 and that at 343 cm^{-1} from ν_4 bending vibrations. For all orthorthombic compounds and the triclinic molybdate fewer bands are observed than expected. Of 20 Raman active modes for the orthorhombic crystals and the triclinic $NaIn(MoO_4)_2$ only 7 are observed for $KIn(WO_4)_2$, 8 for the $KIn(MoO_4)_2$, 10 for the $CsIn(MoO_4)_2$, and 12 for the $NaIn(MoO_4)_2$. The number of recorded IR bands is even smaller than those Raman active. Similar to the case of stretching vibrations, fewer modes are observed because of very small Davydov splitting and the overlapping of weaker oscilators by stronger ones.

The IR and Raman spectra for $LiIn(WO_4)_2$ and $NaIn(WO_4)_2$ differ significantly from the above-described molybdates and tungstate due to the existence of the double oxygen

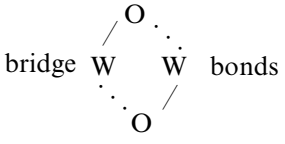

in these crystals. There are $4 \times 3 - 6 = 6$ vibrational modes for a

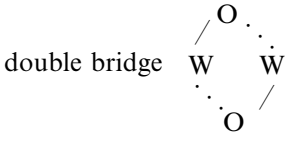

consisting of four atoms. Four of these modes describe stretching and two describe bending vibrations. The remaining $12 - 6 = 6$ modes for each polarization originate from the symmetric stretching (1 mode), asymmetric stretching (1 mode), and bending (4 modes) vibrations of the terminal W–O bonds. The recorded spectra are consistent with the FGA performed for these crystals. Only one very strong Raman band observed at 916 cm^{-1} for $LiIn(WO_4)_2$ originate from the symmetric terminal W–O vibrations and the medium intensity 793 cm^{-1} band with a shoulder at 775 cm^{-1} from the asymmetric W–O vibrations. The four double bridge stretching vibrations are observed in the

528–738 cm^{-1} region. The shoulders at 738 (IR spectrum) and 528 cm^{-1} (Raman spectrum) originate probably from combination modes. The respective spectra of the $NaIn(WO_4)_2$ show the splitting of the $\nu_s(W–O)$ and $\nu_{as}(W–O)$ bands into the two components due to the existence of two different, crystallographically nonequivalent types of oxygen bridges in the crystal structure. The six bending modes are observed in the range 220–500 cm^{-1}.

4.3. External Modes

Translational modes of MoO_4^{2-}, WO_4^{2-}, In^{3+}, and alkali–metal ions as well as librational modes are expected to be observed in the region below 300 cm^{-1}. Former studies of simple tungstates MWO_4, where $M = Ca^{2+}$, Sr^{2+}, Ba^{2+}, and Pb^{2+}, showed that the replacement of a lighter cation by a heavier one results in frequency lowering of the translational modes. The respective modes were observed at 207–210, 162–163, 141–142 and 126 cm^{-1} (33, 36, 39, 52). In the present studies of the trigonal $CsIn(MoO_4)_2$ the broad IR band at 201 cm^{-1} (absent in Raman spectrum) originates from the translations of the In^{3+} ions. The $T'(In^{3+})$ modes for the remaining double molybdates and tungstates are observed in the range 150–243 cm^{-1}, depending on the crystal structure. The translations of caesium ions (atomic mass 133) should be observed at slightly smaller wavenumber that those of In^{3+} ions (atomic mass 115). However, in the crystal lattice of the trigonal and orthorhombic compound the Cs–O bonds are much longer (2.7–3 Å) than those of In–O (2–2.2 Å). Therefore, the $T'(Cs^+)$ translations are observed at much smaller wavenumbers than $T'(In^{3+})$ and were located in the range 80–105 cm^{-1}. For the orthorhombic and monoclinic compounds the frequency of the pure translational vibration is approximately proportional to the square root of the appropriate reciprocal reduced mass. The $T'(K^+)$ modes are observed in the range 143–164 cm^{-1}, $T'(Na^+)$ in the range 197–252 cm^{-1}, and $T'(Li^+)$ at 430 cm^{-1}. Tarte and Liegeois–Duyckaerts (33) observed the translational modes of the MoO_4^{2-} ion in the region 90–140 cm^{-1} and librational modes in the region 180–260 cm^{-1}. The later studies of trigonal molybdates (51, 52) located the translational modes of the MoO_4^{2-} ions in the regions 50–100 and 130–210 cm^{-1}. The librations were located in the 120–170 cm^{-1} range. In the present work for the compounds built up of isolated tetrahedra the librations are observed in the region 140–190 cm^{-1} as medium intensity bands in the Raman spectra and weak bands in IR spectra because the librational vibrations lead to a large change in polarizability. In the case of polymeric $NaIn(WO_4)_2$ and $LiIn(WO_4)_2$ crystals the librational bands are situated below 145 cm^{-1} and should be rather regarded as some kind of torsional movements of chain fragments. The bands originating from translational movements of the MoO_4^{2-} ions are observed for the compounds studied in the 44–148 cm^{-1} wavenumber range and those originating from translational movements of tungstate ions in the range 111–71 cm^{-1}.

This assignment of the vibrational bands to "localized" motions is only an oversimplified scheme. Former results (53, 54) suggest that the translation of the M^+, M^{3+}, and M^{6+} ions are strongly coupled and should be described as mixed $T'(M^+, M^{6+})$ and $T'(M^{3+}, M^{6+})$ translatory lattice modes. In summary, the vibrational properties of the $MIn(MoO_4)_2$ and $MIn(WO_4)_2$ compounds for M = Li, Na, K, Cs have been studied. It was stated that the energy range of stretching vibrations extends from 738 to 992 cm^{-1} and bending from 266 to 462 cm^{-1} for the compounds with tetrahedral coordination of Mo(W) atoms. The respective regions for the polymeric $LiIn(WO_4)_2$ and $NaIn(WO_4)_2$ crystals are larger (498–974 cm^{-1} for the stretching and 213–491 cm^{-1} for the bending modes). The translational and librational modes of the M^+, In^{3+}, WO_4^{2-} and MoO_4^{2-} ions have been observed in the region below 260 cm^{-1}, except for the very light Li^+ ions, for which translational modes were located around 430 cm^{-1}.

REFERENCES

1. J. Hanuza and M. Mączka, *Vibrational Spectrosc.* **7,** 85 (1994).
2. J. Hanuza, M. Mączka, L. Macalik, and J. H. van der Maas, *J. Mol. Struct.* **325,** 119 (1994).
3. J. Hanuza, M. Mączka, and J. H. van der Maas, *J. Phys. Condensed Matter* **6,** 10263 (1994).
4. J. Hanuza, M. Mączka, and J. H. van der Maas, *J. Mol. Struct.* **348,** 349 (1995).
5. J. Hanuza, M. Mączka, and J. H. van der Maas, *J. Solid State Chem.* **117,** 117 (1995).
6. V. A. Efremov, V. K. Trunov, and Yu. A. Velikodnyi, *Zh. Neorg. Khim.* **16,** 1052 (1971).
7. P. V. Klevtsov, R. F. Klevtsova, and A. V. Demenev, *Kristallografiya* **17,** 545 (1972).
8. S. V. Borisov and R. F. Klevtsova, *Kristallografiya* **13,** 517 (1968).
9. P. V. Klevtsov, L. P. Kozeeva, and L. Yu. Kharchenko, *Kristallografiya* **20,** 1210 (1975).
10. R. F. Klevtsova and P. V. Klevtsov, *Kristallografiya* **17,** 955 (1972).
11. R. F. Klevtsova and P. V. Klevtsov, *Kristallografiya* **16,** 292 (1971.
12. L. Yu. Kharchenko and P. V. Klevtsov, *Zh. Noerg. Khim.* **21,** 2836 (1976).
13. V. A. Efremov, V. K. Trunov, and Yu. A. Velikodnyi, *Kristallografiya* **17,** 1135 (1972).
14. A. I. Otko and N. M. Nesterenko, *Ukr. Fiz. Zh.* **24,** 1048 (1979).
15. A. I. Otko, N. M. Nesterenko, and L. P. Povstyanyi, *Phys. Stat. Solidi*(*a*) **46,** 577 (1978).
16. A. I. Otko, N. M. Nesterenko, and A. I. Zvyagin, *Izv. AN SSSR, Ser. fiz.* **43,** 1675 (1979).
17. F. Dudnik, T. M. Stolpakova, and G. A. Kiosse, *Izv. AN SSSR, Ser. fiz.* **50,** 2249 (1986).
18. A. I. Otko, G. G. Krainyuk, T. M. Stolpakova, and E. F. Dudnik, *Izv. AN. SSSR*, Ser. fiz. **48,** 1116 (1984).
19. G. Krainyuk, A. I. Otko, and A. E. osenko, *Izv. AN SSSR, Ser. fiz.* **47,** 758 (1983).
20. P. V. Klevtsov, A. V. Demenev, and R. F. Klevtsova, *Kristallografiya* **16,** 520 (1971).

21. I. G. Avaeva, V. B. Kravchenko, and T. N. Kobyzeva, *Neorg. Mater.* **8,** 586 (1972).
22. V. N. Karpov, I. B. Korotkievich, M. M. Minkova, and O. V. Sorokina, *Zh. Neorg. Khim.* **18,** 1341 (1973).
23. V. B. Kravchenko, *Zh. Strukt. Khim.* **12,** 1108 (1971).
24. P. V. Klevtsov and R. F. Klevtsova, *J. Solid State Chem.* **2,** 278 (1970).
25. Yu. A. Velikodnyi and V. K. Trunov, *Zh. Strukt. Khim.* **12,** 334 (1971).
26. Yu. A. Velikodnyi and V. K. Trunov, *Neorg. Mater.* **10,** 1290 (1974).
27. V. A. Balashov, L. A. Beda, and A. A. Mayer, *Neorg. Mater.* **7,** 334 (1971).
28. V. A. Balashov and A. A. Mayer, *Neorg. Mater.* **7,** 822 (1971).
29. R. H. Busey and O. L. Keller, *J. Chem. Phys.* **41,** 251 (1964).
30. L. A. Woodward and H. L. Roberts, *Trans. Faraday Soc.* **52,** 615 (1956).
31. P. Tartre and J. Predhomme, *Spectrochim. Acta A* **26,** 2207 (1970).
32. P. Tartre and J. Predhomme, *Spectrochim. Acta A* **28,** 69 (1972).
33. P. Tartre and M. Liegeois-Duyckaerts, *Spectrochim. Acta A* **28,** 2029 (1972).
34. A. S. Barker, *Phys. Rev. A* **135,** 742 (1964).
35. G. M. Clark and W. P. Doyle, *Spectrochim. Acta* **22, 1441** (1966).
36. R. K. Khanna and E. R. Lippincott, *Spectrochim. Acta A* **24,** 905 (1968).
37. M. Liegeois-Duyckaerts and P. Tartre, *Spectrochim. Acta A* **28,** 2037 (1972).
38. S. P. S. Porto and J. F. Scott, *Phys. Rev.* **157,** 716 (1967).
39. M. Nicol and J. F. Durana, *J. Chem. Phys.* **54,** 1436 (1971).
40. S. Sheik Saleem, G. Aldruhas, and H. D. Bist, *J. Solid State Chem.* **48,** 77 (1983).
41. S. Sheik Saleem, G. Aldruhas, and H. D. Bist, *Spectrochim. Acta A* **39,** 627 (1983).
42. S. Sheik Saleem, G. Aldruhas, and H. D. Bist, *Spectrochim. Acta A* **39,** 1049 (1983).
43. S. Sheik Saleem, G. Aldruhas, and H. D. Bist, *Spectrochim. Acta A* **40,** 149 (1984).
44. S. Sheik Saleem, G. Aldruhas, and H. D. Bist, *Infrared Phys.* **23,** 217 (1983).
45. S. Sheik Saleem and T. K. K. Srinivasan, *Spectrochim. Acta A* **41,** 1419 (1985).
46. W. P. Griffith, *J. Chem. Soc. A* 211 (1969).
47. J. Hauck and A. Fadini, *Z. Naturforsch. B* **25,** 422 (1970).
48. M. Liegeois-Duyckaerts and P. Tarte, *Spectrochim. Acta A* **30,** 1771 (1974).
49. A. Müller, E. J. Baran, and R. O. Carter, *Struc. Binding* **26,** 81 (1976); and references cited therein.
50. M. Maczka, *Eur. J. Solid State Inorg. Chem.* **33,** 783 (1996).
51. N. M. Nesterenko, V. I. Fomin, and V. I. Kutko, *Fiz. Niz. Temp.* **8,** 862 (1982).
52. V. V. Fomichev, V. A. Efremov, D. D. Baldanova, I. O. Kondratov and K. I. Petrov, *Zh. Neorg. Khim.* **28,** 1184 (1983).
53. J. Hanuza and L. Macalik, *Spectrochim. Acta A* **43,** 361 (1987).
54. V. V. Fomichev and O. I. Kondratov, *Spectrochim. Acta A* **50,** 1113 (1994).